Journal Pre-proofs

Full length article

Molecular mechanistic insights towards aggregation of nano-biochar moderated by aromatic components in dissolved organic matter

Zheng Zhou, Meng Lu, Yu Huang, Changping Zhao, Yafeng Wang, Marc Pidou, Min Wu, Quan Chen, Paul Jeffrey, Bo Pan

PII: S0160-4120(25)00101-1
DOI: https://doi.org/10.1016/j.envint.2025.109350
Reference: EI 109350

To appear in: *Environment International*

Received Date: 11 December 2024
Revised Date: 22 February 2025
Accepted Date: 22 February 2025

Please cite this article as: Z. Zhou, M. Lu, Y. Huang, C. Zhao, Y. Wang, M. Pidou, M. Wu, Q. Chen, P. Jeffrey, B. Pan, Molecular mechanistic insights towards aggregation of nano-biochar moderated by aromatic components in dissolved organic matter, *Environment International* (2025), doi: https://doi.org/10.1016/j.envint.2025.109350

Molecular mechanistic insights towards aggregation of nano-biochar moderated by aromatic components in dissolved organic matter

Zheng Zhou[1], Meng Lu[1, 2], Yu Huang[1, 3, *], Changping Zhao[1], Yafeng Wang[1], Marc Pidou[3], Min Wu[1], Quan Chen[1, *], Paul Jeffrey[3], Bo Pan[1]

[1] *Yunnan Provincial Key Lab of Soil Carbon Sequestration and Pollution Control, Faculty of Environmental Science & Engineering, Kunming University of Science & Technology, Kunming 650500, Yunnan, China;*

[2] *School of Environmental Studies, China University of Geosciences, Wuhan 430074, Hubei, China;*

[3] *Cranfield Water Science Institute, Cranfield University, Cranfield, United Kingdom.*

* Corresponding authors:

Yu Huang, E-mail: yuzhehy@qq.com

Quan Chen, E-mail: 18814122937@163.com

Abstract:

Nano-biochar (NBC) is a promising tool for sustainable remediation of contaminants in aquatic environments. However, the presence of ubiquitous ions and dissolved organic matter (DOM) can impact NBC aggregation, resulting in reduced application efficacy and potential ecological risks. Understanding and regulating NBC aggregation offers valuable insights for its deployment. This study integrated batch aggregation experiments, theoretical models, Fourier transform ion cyclotron resonance-mass spectrometry (FTICR-MS), and density functional theory (DFT) calculations to explore the behaviors and mechanisms of NBC aggregation with coexisting ions and model DOM. NBC aggregation kinetics followed the classical Derjaguin-Landau-Verwey-Overbeek (DLVO) theory in both NBC-ions and NBC-ions-fulvic acid (FA) solutions, indicating that the aggregation process is controlled by Van der Waals forces and electrostatic repulsion. Mono/di-valent electrolytes promoted NBC aggregation, whereas FA moderated it, with higher molecular weight

FA fractions exhibiting superior performance. Three-dimensional excitation-emission (3D-EEM) fluorescence spectra and Parallel factor analysis (PARAFAC) analyses revealed that HA-like substances, followed by FA-like substances, can form a complex with ions, thereby moderating NBC aggregation. FTICR-MS scans identified lignin substances with aromatic structures as key components that effectively reduce the promoted NBC aggregation with coexisting mono/di-valent electrolytes. DFT calculations confirmed that the aromatic structures in FA spontaneously form complexes with electrolytes, thereby potentially regulating NBC aggregation. This research highlights potential strategies for regulating NBC applications and offers insights into the behavior of nanoparticles in aquatic environments.

Keywords: Nanoparticles; Complexation; Fourier transform ion cyclotron resonance-mass spectrometry; Aggregation moderation; Dissolved organic matter.

1. Introduction

Nano-biochar (NBC), an advanced carbon-based nanomaterial, exhibits distinctive physiochemical characteristics, including a large surface area, high catalytic reactivity, and diverse crystalline forms (Hagemann et al., 2017; Lian et al., 2022; Shao et al., 2021). These unique features make NBC a promising candidate for various aquatic environmental applications, for example, eliminating trace organic pollutants (Qiu et al., 2022; Song et al., 2024), carrying advanced oxidation catalyst (Naghdi et al., 2018), and stunning soil heavy metals (He et al., 2022). Similar to other nanoparticles, the high surface energy of NBC facilitates its rapid aggregation upon application in aquatic environments (Song et al., 2022).

Extensive literature demonstrates the crucial role of NBC aggregation in regulating its functioning efficacy and transporting behavior, thereby determining the corresponding environmental fate and risk (Lian et al., 2024). The aggregated NBC results in reduced catalysis, sorption, and electron shuttle performance (Jin et al., 2022), hence significantly restricts its functioning efficacy. For example, NBC aggregation reduces removal performance for treating organic pollutants due to the decreased sorption capacity and degradation efficiency. As particle concentration increases, the exposed surface area ratio in the aqueous phase decreases from 0.46 to 0.05 (Xing et al., 2023). Since NBC has a strong affinity for heavy metals and organic pollutants, the migration of these aggregates may pose ecological risks to groundwater and soil aquifers (Liu et al., 2020; Naghdi et al., 2017). Therefore, understanding mechanisms that determine NBC aggregation can enable precise regulation in case-by-case applications, also maximizing practical efficacy and minimizing potential

risks.

NBC will inevitably interact with inorganic and organic compounds in the natural environment during application (Liu et al., 2018). These complicated interactions can lead to varied aggregation behaviors by altering its surface properties, electrostatic repulsion, and steric interaction (Singh et al., 2021). Recent advances have identified parameters that determine NBC aggregation, including pH (Liu et al., 2022), coexisting ions (Chen et al., 2017), dissolved organic matter (DOM) (Jiang et al., 2023), and root exudates (Zhang et al., 2022). Among these factors, cations can promote NBC aggregation by reducing the electrostatic repulsive interactions and charge screening effects (Li et al., 2017), pH influences NBC aggregation through changes in zeta potential (Lian et al., 2020), while the negatively charged humic acid (HA) may prevent the NBC aggregation by weakening the interactions of electric double layers on the particle surface (Xu et al., 2021). However, the complexations between organic and inorganic compounds in actual environments are often overlooked, particularly in scenarios where NBC coexists with both ions and DOMs. Indeed, the ions universal presence in the natural environments can complex with DOMs (D.Schmitt 2002), potentially impacting NBC aggregation. In addition, the molecular weight (MW) of NOMs has been shown to indicate their composition, chemical structure, and reactivity (Chen et al., 2021).

In complicated aquatic environments, the types and concentrations of ions, as well as the sources, structural compositions, and MW of DOMs, require investigation of NBC aggregation in NBC-ions-DOMs ternary systems. To improve the limited resolution in bulk organic analysis, Fourier transform ion cyclotron resonance mass spectrometry (FTICR-MS) offers ultra-high resolution for molecular-level characterization of DOM (Li et al., 2016). By such an approach, DOM variations in different river flows can be classified into unsaturated compounds in headwaters and aliphatic molecules at downstream sites (Norbert et al., 2019). Conversely, theoretical calculations using density functional theory (DFT) have been shown to elucidate molecular interactions from a quantum chemical perspective (Lu et al., 2022). For instance, Lu et al. quantified the interaction mechanisms, intermolecular forces, and adhesion energies between two humic acids and divalent cations (Mg^{2+}, Ca^{2+}, Zn^{2+}, Cu^{2+}) in an aqueous environment (Lu et al., 2023). Therefore, combining advanced mass spectrometry measurements with theoretical calculations provides a promising approach to understanding NBC aggregation in the presence of ions and NOMs, offering insights into potential regulatory strategies for precise NBC applications.

This study thus comparatively investigates the aggregation behaviors of NBC in the presence of $Na^{+}/Ca^{2+}/Cl^{-}/SO_4^{2-}$ ions, as well as in NBC-ions-DOMs systems. Fulvic acid (FA), representing DOM, was fractionated into five MW ranges (<500, 500-1000, 1000-3500, 3500-7000, and >7000 Da), and added to the binary NBC-ion systems. Time-resolved dynamic light scattering (TR-DLS) and Deryagin-Landau-Verwey-Overbeek (DLVO) calculations were used to analyze NBC aggregation

behavior. Bulk organic variations were monitored through total organic carbon, ultraviolet, and fluorescence spectra to reveal the macroscopic mechanisms of NBC-ions-DOM aggregation. FTICR-MS scans and DFT calculations were performed to elucidate the molecular-scale mechanisms. Future perspectives on NBC implementation are discussed, with case-by-case schemes provided. This study expands the understanding of NBC aggregation in natural environments and proposes potential regulatory strategies for efficient nano-biochar applications with minimized ecological risks.

2. Materials and methods

2.1 Preparation of nano-biochar, regents, and fulvic acid fractionated samples

Nano-biochar (NBC) was prepared from corn stalk and nano-sized using a planetary activator (Sky Creator XQM-04L, China). Sodium chloride (NaCl), Calcium chloride ($CaCl_2$), and Sodium sulfate (Na_2SO_4) solutions representing the presence of typical monovalent (Na^+, Cl^-) and divalent (Ca^{2+}, SO_4^{2-}) ions in the natural environment were purchased from Aladdin Reagent (Shanghai, China) with at least analytical grade. Fulvic acid (FA) representing the NOMs was purchased from Macklin Biochemical Technology (Shanghai, China) with a ≥ 95% purity. Raw FA sample was fractionated by dialysis filtration into five molecular weights: FA-1 (≤ 500 Da), FA-2 (500 - 1000 Da), FA-3 (1000 - 3500 Da), FA-4 (3500 – 7000 Da), and FA-5 (≥ 7000 Da). All experiments were conducted using ultrapure (UP) water (ELGA Milli-Q, USA). Details about NBC preparation, fractional separation, and corresponding elemental composition of FA samples can be found in **Section S1-3**.

2.2 Aggregation kinetic experiments

The aggregation of NBC was investigated in the binary and ternary matrices of NBC-ions and NBC-ions-FA, respectively. According to previous studies (Wang et al., 2019; Yang et al., 2022) and our pre-test results, to obtain the exact critical coagulation concentration (CCC) in both NBC-ions and NBC-ions-FA solutions, 1mg NBC was dosed into a glass beaker and kept stirred with variable ion strength solutions and FA fractions until sampled for analytical measurement. For NBC-ions trials, 1 mg NBC was added into 20 mL NaCl, $CaCl_2$, and Na_2SO_4 solutions, respectively. For NBC-ions-FA trials, based on the critical concentration of reaction-limited aggregation and diffusion-limited aggregation (DLA) stages obtained in the binary tests (Huguet et al.,), 10 mL ion solutions were mixed with 10 mL FA solutions to ensure the concentration of reaction solution is 5 mg C/L. Then, NBC was added to the ions-FA solution and performed the aggregation test. Each aggregation experiment was conducted in triplicate. Detailed dosing schemes in this study are displayed in **Table 1**.

Table 1. Cations, anions, and fulvic acid dosing scheme in this study.

Binary systems	
Ion solution	Concentration (mM)
NaCl	0, 10, 50, 100, 200, 300, 500, 700, 900, 1000
$CaCl_2$	0, 1, 4, 10, 20, 30, 40, 60, 80, 100, 150, 200
Na_2SO_4	0, 5, 10, 50, 100, 250, 500, 1000

Ternary systems				
Stage	Ion solution	Concentration (mM)	Fulvic acid fraction molecular weight (Da)	Reaction Solution TOC Concentration (mg C/L)
No ions	NaCl	0	FA-1(<500)	5
	$CaCl_2$	0		
	Na_2SO_4	0		
RLA	NaCl	300	FA-2(500-1000)	
	$CaCl_2$	4	FA-3(1000-3500)	
	Na_2SO_4	50	FA-4(3500-7000)	
DLA	NaCl	500	FA-5(>7000)	
	$CaCl_2$	40		
	Na_2SO_4	200		

Notes: RLA: Reaction-limited aggregation stage; DLA: Diffusion-limited aggregation stage.

2.3 Analytical measurements and data analysis

The aggregation experiments were carried out by using Zeta Sizer Nano ZS90 (Malvern Instrument, UK) with a 640 nm laser wavelength and a He-Ne laser with a scattering angle of 90° and a test temperature set at 25 °C. NBC's hydrodynamic diameter and zeta potential were measured using a size and zeta potential analyzer (Brookhaven Instruments Corporation, US) at pH 7.0 and a refractive index of 1.50. For macroscopic aggregation behavior analysis, DLVO theory was applied to describe the obtained kinetics and determine the homotypic coalescence of NBC. The stability curve of NBC was fitted, and the Hamaker constant was calculated. The interaction energy between NBC was calculated with a sphere-sphere configuration as van der Waals attraction (V_{VDW}) and electrical double-layer repulsion (V_{EDL}). The critical coagulation concentration (CCC) was obtained to indicate the transition point between the RLA and DLA stage. Total organic carbon (TOC) was measured with a Vario TOC analyzer (Elemental, Germany) to determine the variation of Fulvic acid (FA) during the aggregation process. Bulk molecular structures of FA samples were determined by an ultraviolet-visible spectroscopy (UV-Vis) (Evolution 201, Thermo Fisher Scientific, USA). Organic composition in the NBC-ions-FA trials was evaluated by a fluorescence spectrometer (F-7000, Hitachi, Japan) with 3D excitation-emission matrices(3D-EEM). Results from the fluorescence spectrometer were plotted as a 2D intensity map, and the fluorescence regional integration (FRI) analysis was extracted with the OpenFluor platform. FTICR-MS was applied to each fractionated FA sample to enhance the limited resolution of FA's composition determination and reveal the structural regulation mechanisms in NBC-ions-FA aggregation progress. Detailed analytical measurement procedures include UV-Vis, 3D-EEM fluorescence spectra and PARAFAC analysis, FTICR-MS, the CCC and DLVO related calculations can be found in **Section S4-8**.

2.4 Quantum chemical calculations

Insights into molecular interactions between ions and FA fractions were investigated and visualized using DFT calculations in Material Studios 2019. Model molecules were constructed according to the results from PARAFAC analysis, FTICR-MS, and reported literature (Devarajan et al., 2020; Yang et al., 2020). Ten molecular structures representing 5 organic matters (Fulvic Acid, Humic Acid, D-tryptophan, Tyrosin, and Lignins) were selected as model structures. Detailed DFT calculation parameters are shown in **Section S9.**

3. Results and discussion

3.1 Coexisting mono/di-valent electrolytes promoted NBC aggregation

The variation in distinctive hydraulic diameter (D_h) observed in **Figures 1(a)-(c)** suggests that different electrolytes significantly altered the NBC aggregation. At low electrolyte concentrations of ≤ 10 mM NaCl, ≤ 20 mM $CaCl_2$, and ≤ 5 mM Na_2SO_4,

the D_h of NBC remained stable at around 300 nm, suggesting minimal particle aggregation. In contrast, higher ion concentrations led to an increased D_h up to 1200 nm, 1100 nm, and 1000 nm in NaCl, $CaCl_2$, and Na_2SO_4 solutions, respectively, indicating an intensified NBC aggregation, primarily due to the compressed double layers and neutralization of ions in these ranges. Notably, no further increase in D_h was observed at electrolyte concentrations exceeding ≥ 500 mM NaCl, ≥ 80 mM $CaCl_2$, and ≥ 100 mM Na_2SO_4. However, the D_h of Na_2SO_4 solutions showed a negligible increase in 250 mM and 500 mM but a slight increase in 1000 mM compared to the 100 mM. This suggests that increasing the Na_2SO_4 concentration after 100 mM had a limited promoting effect on NBC aggregation due to the compressed electric double layers and the approached critical aggregation concentration (Yang et al., 2022). In contrast, the minor increase at 1000 mM may be attributed to the co-precipitation and bridging effects in high-concentration ion solutions (Rosenberg et al., 2011). Furthermore, the comparison of D_h in different ion solutions supports previous findings that divalent ions exhibited a more substantial effect on promoting NBC aggregation than monovalent ions (Gao et al., 2017). At the same molar concentration, the divalent ions induce the NBC aggregation *via* strong complexing due to a more intense charge density in the diffusion layer, thus more effectively reducing the aggregation energy barrier than electric double layer suppression caused by monovalent ions (Lin et al., 2023).

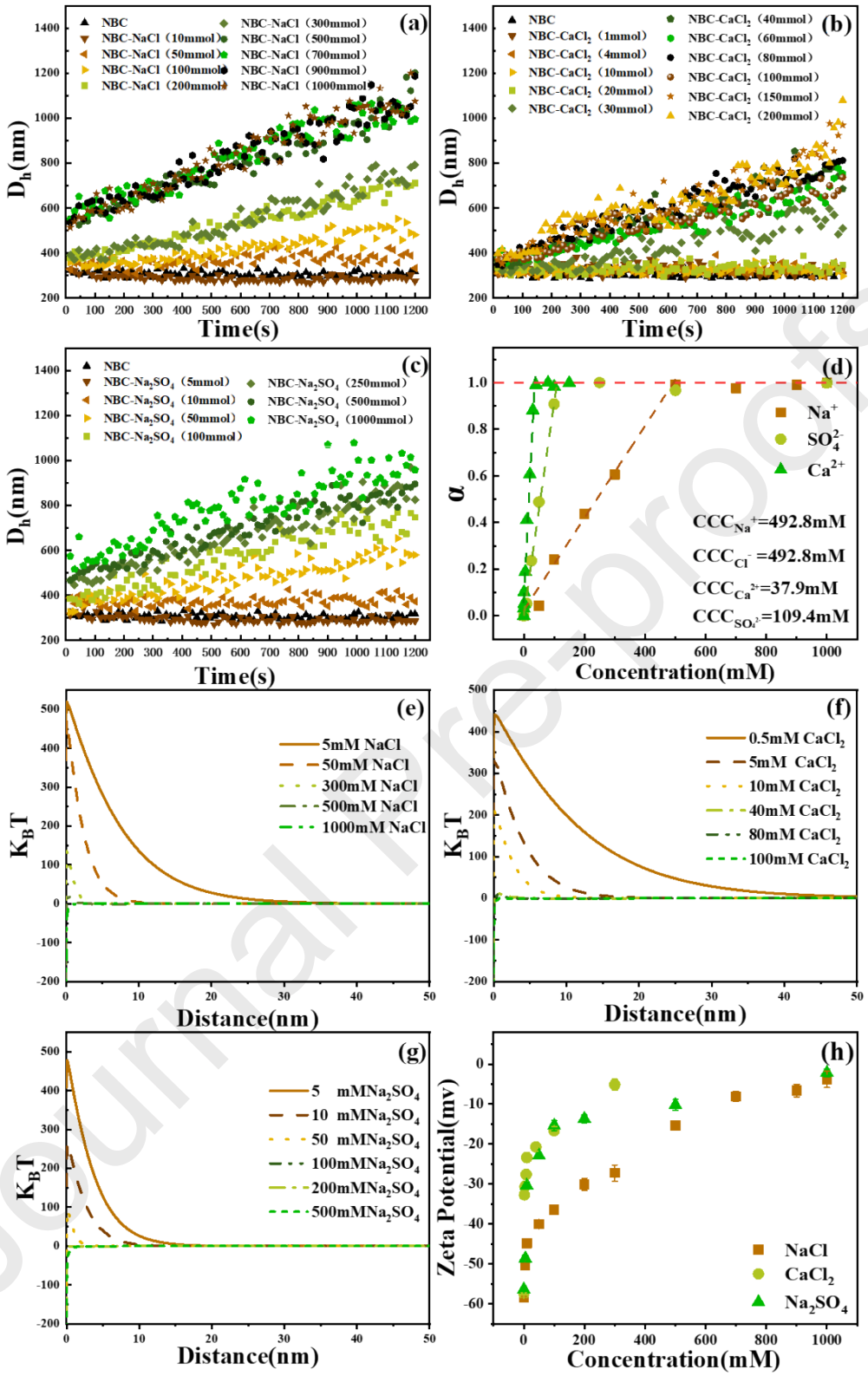

Figure 1. Hydraulic diameters (D_h) of NBC in NaCl (a), $CaCl_2$ (b), and Na_2SO_4 (c) solutions with varying ion concentrations; Critical coagulation concentration (CCC) of NBC in different ion solutions (d); Relationship between normalized DLVO interaction energy (K_BT) curve and separation distance of NBC in NaCl (e), $CaCl_2$ (f), and Na_2SO_4 (g) solutions; Zeta potential of NBC in different ion solutions (h).

DLVO theory calculation was employed to emphasize the aggregation kinetic behaviors of NBC. **Figure 1(d)** illustrates the sticking efficiency (α) profiles of NBC in three ion solutions. The critical coagulation concentration (CCC) of NBC in Na^+/Ca^{2+} and Cl^-/SO_4^{2-} ion solutions are 492.8 mM Na^+/Cl^-, 37.9 mM Ca^{2+} and 109.4 mM SO_4^{2-}, respectively. The minor difference with the D_h results that consequently, the NBC aggregation can be divided into two stages: reaction-limited aggregation (Huguet et al.,) stage and diffusion-limited aggregation (DLA) stage(Lin et al., 1990). In the RLA stage, α increases with rising ion concentration until it surpassed the CCC, at which point the maximum aggregation rate is reached and α approaches 1. The aggregation rate *K* subsequently displayed no further increase, indicating a transition to the DLA stage. This shift can be attributed to the greater electrostatic repulsion compared to van der Waals forces among NBC particles at low ion concentrations (Hu et al., 2021). The accelerated aggregation rate was consistent with increasing ion concentrations. It has been noted that Cl^- can interfere with hydrogen bonds between water molecules, weakening the stability of hydrophobic interaction, thus inhibiting the aggregation of NBC in aqueous solution (Fang et al., 2013). However, in this study, the coexistence of Na^+/Ca^{2+} resulted in a continuous increase in NBC aggregation with increasing ion concentrations, indicating that cations may play a more crucial role in regulating the NBC aggregation by neutralizing the negative surface charges. According to the different CCC values in each ion solution, the following order of effectiveness in promoting NBC aggregation was established: Ca^{2+} (37.9 mM) > SO_4^{2-} (109.4 mM) > Na^+ (492.8 mM) ≥ Cl^- (492.8 mM).

This highlights two critical electrolyte concentration thresholds that should be considered when studying NBC aggregation. Furthermore, a comparison of D_h in different ion solutions reveals that divalent ions exhibited a more substantial effect on promoting NBC aggregation than monovalent ions, possibly due to their higher charge density in the diffusion layer at the same molar concentration, reducing the energy barrier for aggregation more effectively than monovalent ions (Lin et al., 2023).

Figures 1 (e)-(g) display the relationships between DLVO interaction energy and particle distance of NBC in NaCl, $CaCl_2$, and Na_2SO_4 solutions. As the concentrations of NaCl, $CaCl_2$ and Na_2SO_4 increase, the total interaction energy (V_T) decreased with the increasing distance (*h*) between NBC particles. This complied with the sticking efficiency profiles (**Figure 1(d)**) that the V_T gradually decreased to 0 with the increasing ion concentration in the RLA stage, subsequently stabilizing in the DLA stage. This is attributed to the reduced surface potential of NBC, which lowers the energy barrier and promotes aggregation (Wang et al., 2022). In the DLA stage, the energy barrier between NBC is entirely eliminated, resulting in a maximum aggregation rate(TANAPON et al., 2007). Therefore, DLVO calculations demonstrated the critical concentrations for achieving zero V_T, hence shifting to the DLA stage, are 492.8 mM for NaCl, 37.9 mM for $CaCl_2$, and 109.4 mM for Na_2SO_4, respectively.

Figure 1(h) shows the variation of zeta potential on the surface of NBC under different ion concentrations. The zeta potential of NBC in water was determined as -58.42 ± 0.25 mV. As expected, the absolute zeta potential of NBC decreased with the increasing NaCl, $CaCl_2$, and Na_2SO_4 concentrations. This is consistent with the DLVO analysis and confirms the neutralization effect of negative charges on the surface of NBC after adding counter ions. Notably, Ca^{2+} exhibited a more significant neutralization effect than other ions, resulting in an undetectable D_h in the aggregation kinetic experiment (300 mM $CaCl_2$), consistent with a previous study (Huang et al., 2013). In contrast, SO_4^{2-} exhibited a limited electrostatic shielding effect compared to Cl^-, possibly because of the electrostatic repulsion between the negative charges on both the NBC surface and these two anions (Gao et al., 2017). Additionally, SO_4^{2-} enhances the interaction between water molecules, which increases the hydrophobic interaction among NBC particles, further promoting their aggregation (Yang et al., 2022).

3.2 Fulvic acid moderates NBC aggregation promoted by coexisting electrolytes

The aggregation kinetics of NBC-ions-FA ternary solutions are displayed in **Figures 2(a)-(f)**. Distinctive aggregation of NBC was observed in all trials without FA addition. The introduction of FA significantly mitigated NBC aggregation, especially the FA with higher MW enhanced this mitigation effect. This could be attributed to the enhanced electrostatic and spatial repulsion effects of FA molecules (Wang et al., 2013b). With the addition of FA-5, the aggregation rate of NBC remained nearly zero, and the D_h stabilized around 300 nm throughout the observation period. This is also confirmed by the RLA stage and DLA stage in **Figures 2(h)-(g)**, the surface negative charge of NBC increased upon FA addition, while the surface negative charge increased with the increasing FA MW. Compared to the binary systems, the addition of FA resulted in a distinctive increase in zeta potential for ternary systems, regardless of the DLA and RLA stages.

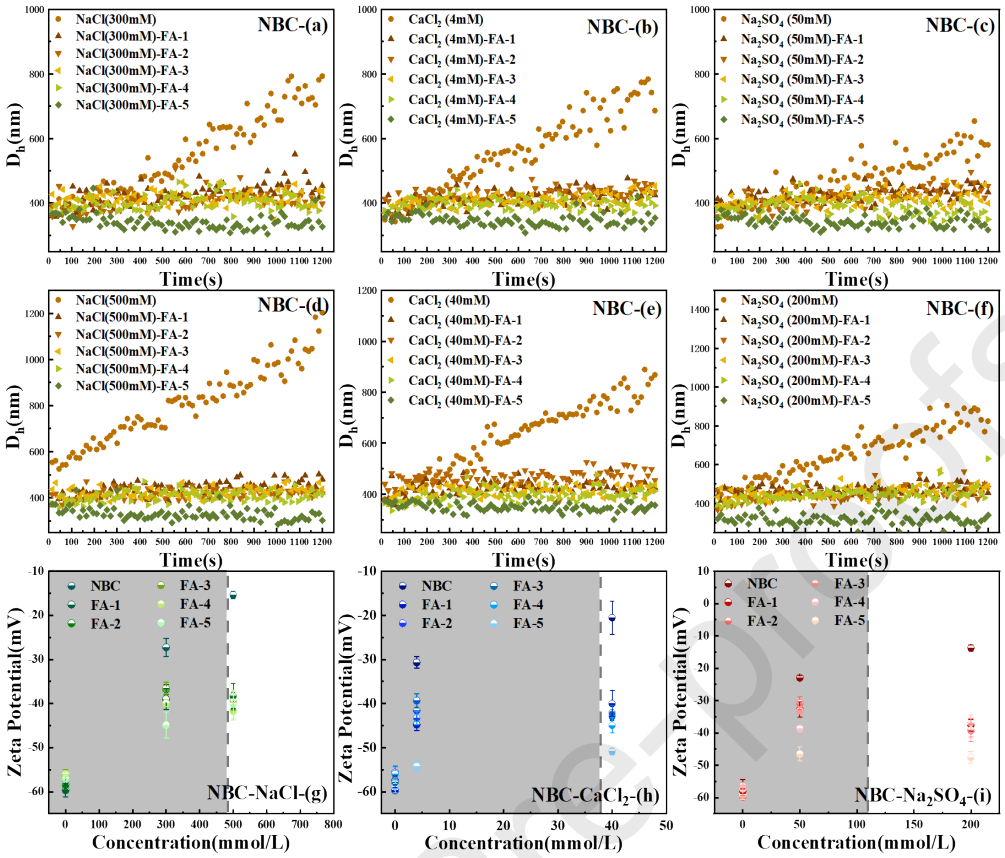

Figure 2. Hydraulic diameters (D_h) of NBC in 300 mM NaCl (a), 4 mM $CaCl_2$ (b), 50 mM Na_2SO_4 (c), 500 mM NaCl (d), 40 mM $CaCl_2$ (e) and 200 mM Na_2SO_4 (f) solutions with different molecular weight fulvic acid; Zeta potential of NBC in varying concentrations of NaCl (h), $CaCl_2$ (g), Na_2SO_4 (i) solutions with different molecular weight fulvic acid, the gray and white mean RLA and DLA stage, respectively.

The comparison of binary NBC-ion and ternary NBC-ion-FA solutions partially elucidates the mechanism by which FA reduces NBC aggregation. The FA molecules enhance the electrostatic repulsion and steric hindrance effect between NBC. Moreover, the constant addition of FA to the solution confirms the aggregation-promoting ability observed for various ions in binary solution experiments. Consequently, the differing mitigation performances of five FA fractions attracted us to further investigate the structural regulatory mechanisms of NBC aggregation in the NBC-ions-FA systems.

3.3 Humic acid-like and fulvic acid-like substances effectively moderate the promoted aggregation in NBC-ion solutions

The absorbance-wavelength curves (**Figure S1**) of five FA fractions with different MWs exhibited similar absorption behaviors. **Figure S2** displays the variation in TOC in the NBC-ion-FA ternary system during the 20-minute observation

period. A sharper decrease in residual TOC was observed accompanied by the addition of higher MW FA fractions, which can be attributed to the complexed FA molecules and ions being adsorbed onto the surface of NBC. Indeed, the FA consumption increased correspondingly with the increase in ion concentration, and the amount of FA consumed positively correlated with the MW. This confirms that the FA fraction with higher MW demonstrated superior performance in mitigating NBC aggregation in the ternary systems. The 3D-EEM fluorescence spectra of the ternary solutions before and after the aggregation experiments are presented in **Figure 3**. Raw FA fractions exhibit three characteristic peaks that are consistent with varying MWs. Peak A representing protein-like substances at Ex (230-235, 275-280 nm) / Em (310-340 nm), peak B representing humic acid-like substances at Ex (275-280 nm) / Em (385-405 nm), and peak C representing fulvic acid-like substances at Ex (230-240 nm) / Em (390 nm). Compared to raw binary solutions, the solutions with added fractionated FA showed a clear shift from humic acid-like towards protein-like and fulvic acid-like substances peaks in FA-2, FA-3, FA-4, and FA-5. In contrast, no clear peak shifts were observed in the FA-1 solution. However, minimal variation was observed in the fluorescence index (FluI), freshness index (FrI), biological index (BIX), and humification index (HIX) (**Table S2**).

Table S3 lists the UV-Vis spectral characteristics of the MW-fractionated FA components in this study. The aromatization decreases with increasing molecular weight. The classified Humification index (HIX) shows that the humification degree of each FA increased with higher MW. The decrease in humification with increasing molecular weight may be due to the condensation of the benzene ring and the introduction of other non-aromatic functional groups, which decrease the overall aromaticity of the substance (Wei et al., 2022).

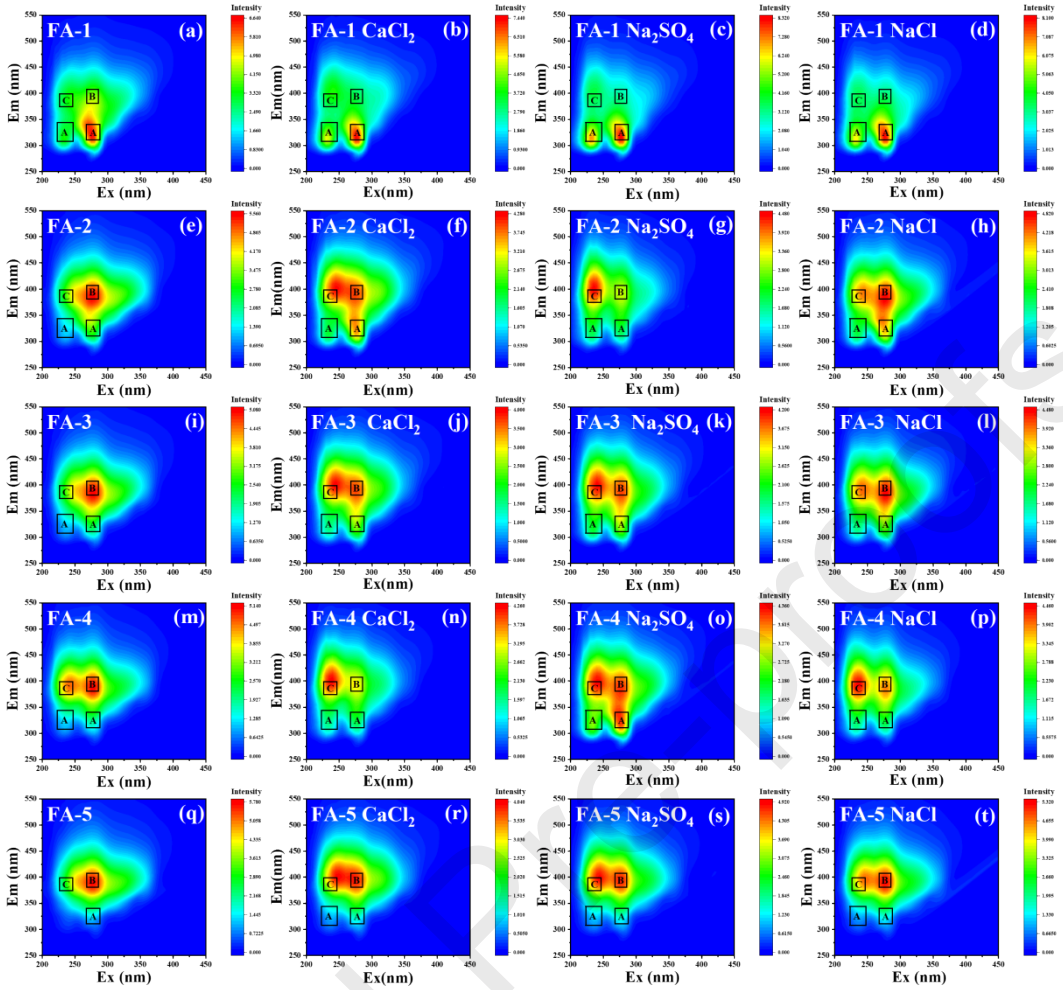

Figure 3. Piloted three-dimensional fluorescence spectra of FA sample with five MWs, FA-1 (a), FA-2 (e), FA-3 (i), FA-4 (m), FA-5 (q); Piloted three-dimensional fluorescence spectra of NBC-ions-FA after the aggregation experiments. The corresponding solution matrix was marked at the top of each spectra map. For example, FA2 $CaCl_2$ (f) represents the spectra of the NBC-$CaCl_2$-FA-2 solution after the aggregation experiment.

Parallel factor analysis (PARAFAC) was employed to better understand the 3D-EEM data and elucidate the potential regulatory mechanisms in the ternary systems. The results clearly indicated two fluorescent components in FA-1, FA-3, FA-4, and FA-5 samples, with only one component identified for FA-2. The identified components were validated through split-half testing and residual analysis (**Table S4**). Subsequently, the variation of FA components during the NBC-ions-FA aggregation experiment was identified and is displayed in **Figure 4**.

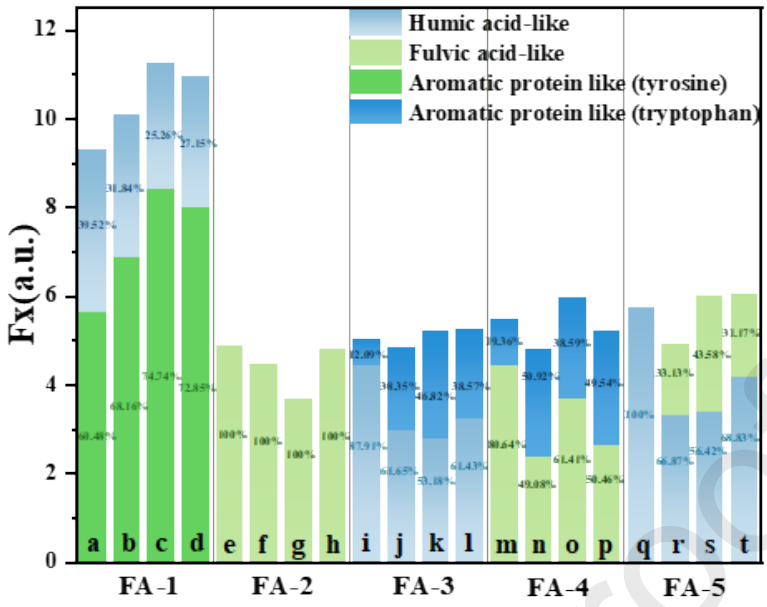

Figure 4. Identified organic components in FA-1 (a), FA-2 (e), FA-3 (i), FA-4 (m), and FA-5 (q) samples; Identified organic components of NBC-ions-FA solutions after the aggregation experiments. In which, FA-1 (b), FA-2 (f), FA-3 (j), FA-4 (n), FA-5 (r) are in $CaCl_2$ solutions; FA-1 (c), FA-2 (g), FA-3 (k), FA-4 (o), FA-5 (s) are in Na_2SO_4 solutions; and FA-1 (d), FA-2 (h), FA-3 (l), FA-4 (p), FA-5 (t) are in NaCl solutions.

The FA fraction with a MW less than 500 Da exhibited the highest fluorescence intensity after the aggregation process, correlating with the lowest decrease in TOC. The integrated fluorescence intensities of all NBC-ions-FA-1 solutions are higher than the raw FA-1 sample, possibly due to the altered solution ionic environment. Since the D_h of particle remained nearly stable and the TOC exhibited a minor decrease in NBC-ions-FA-1 solutions, this suggests that HA-like and aromatic protein-like (tyrosine) substances with small molecular weights (< 500 Da) might only complex with ions but not bridge to NBC. In contrast, the other FA fractions reflected much lower intensities with distinctive variation after the aggregation process. This complies with the TOC variations, also argues that FA fractions with a MW larger than 500 Da may complex with ions and then bridge to the NBC, leading to the distinctive reduction in the remaining amounts of organic matter. The aromatic protein-like content in the NBC-ions-FA-2 solutions showed a slight reduction in the remaining solutions compared to the raw FA-2 sample, which requires further investigation. In contrast, in solutions with the addition of FA-3, FA-4, and FA-5, the fulvic acid-like (FA-4) and humic acid-like (FA-3 and FA-5) substances gradually decreased while the aromatic protein-like substances significantly increased after the aggregation process. The FA fractions in those trials changed from humic acid-like and fulvic acid-like substances to aromatic protein-likes, suggesting that humic acid-like followed by fulvic acid-like substances are the primary functional organic matter in NBC-ions-FA solutions for effective NBC aggregation mitigation.

3.4 Molecular insights into aggregation mechanisms in NBC-ions-FA solutions

The bulk organic analyses highlighted the critical roles that humic acid-like and fulvic acid-like substances play in the NBC aggregation in the presence of ions. To elucidate structural regulatory mechanisms associated with different organic components linked to each FA fraction, FTICR-MS scan results are emphasized and displayed in **Figure 5 (a)-(e)**. All identified molecules were plotted in the van-Krevelen diagram and classified as lipids, proteins, aminosugars, carbohydrates, condensed hydrocarbons, lignin, and tannin compounds (Maizel et al., 2017).

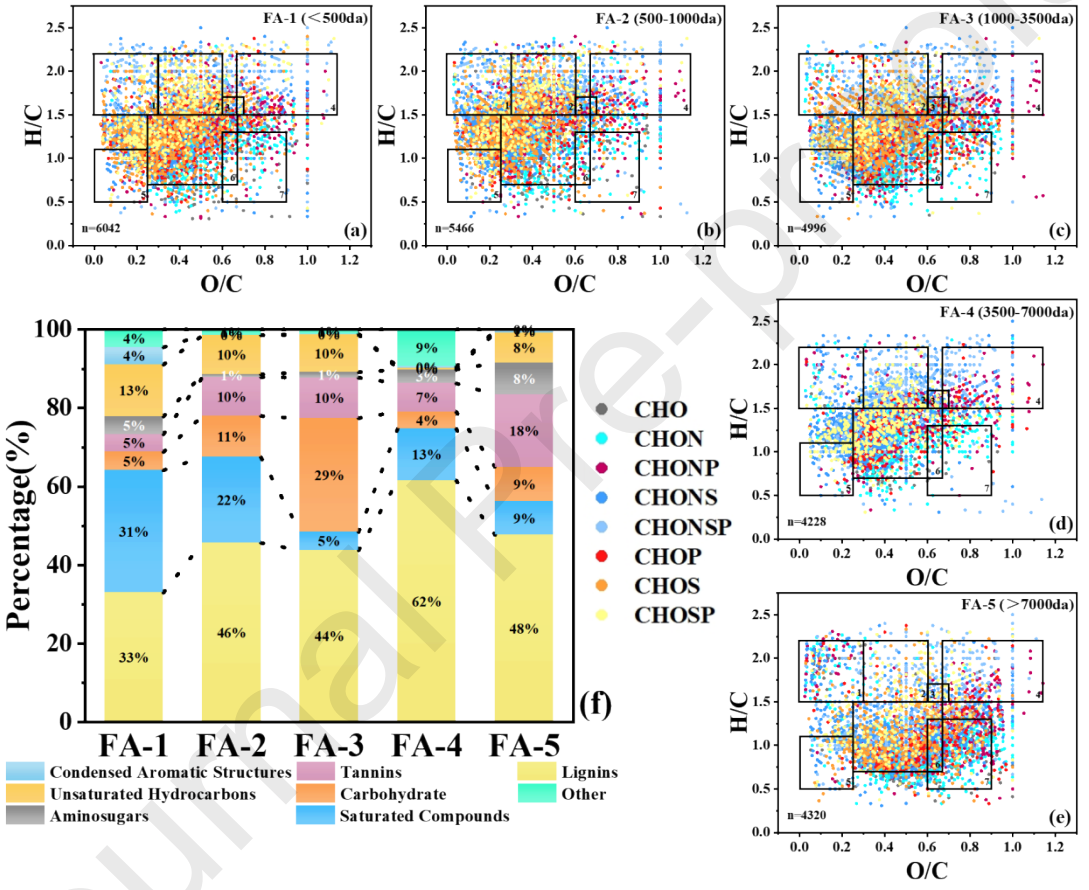

Figure 5. Van Krevelen diagram of FA-1 (a), FA-2 (b), FA-3 (c), FA-4 (d) and FA-5 (e). The rectangles indicate regions associated with lipids (1), proteins (2), aminosugars (3), carbohydrates (4), condensed hydrocarbons (5), lignin (6), and tannin (7); Proportional distributions of identified molecules in each FA samples (f).

Among the five FA fractions, FA-1 exhibited the highest levels of saturated compounds (31%) and unsaturated hydrocarbons (13%), but the lowest content of lignin (33%) and tannin (5%). This suggests that the saturated compounds and unsaturated hydrocarbons may lack sufficient reactivity to complex with ions and bridge to biochar, resulting in reduced mitigation performance in the ternary aggregation trials. In addition, the vigilantly varied amounts of carbohydrates (4%-

29%) suggest their negligible contribution to mitigation in the ternary solutions. For FA-2, FA-3, FA-4, and FA-5, the low content of condensed aromatic structures indicated its minor role in complexation with ions. In contrast, the significantly higher levels of lignin (44%-62%) and tannin (7%-18%) substances in these four FA fractions underscore their critical roles in effective ion complexation and mitigating NBC aggregation in the ternary solutions. Moreover, regarding the complexation selectivity towards different ions, the highest lignin content (62%) found in FA-4 among all FA fractions highlights its crucial role in reducing NBC aggregation. In comparison, the 7%-10% unsaturated hydrocarbons present in FA-2, FA-3, and FA-5 significantly improve the mitigation performance, whereas FA-4 contains nearly none. Since FA-4 showed less effective regulation than FA-2 and FA-3 regardless of the NBC-ion matrixes, this highlights the potential directional regulation of NBC aggregation with unsaturated hydrocarbons.

In combination with the PARAFAC results, this highlights the potential application strategy of adjusting the unsaturated hydrocarbons in the humic acid-like substances to provide directional regulation of NBC aggregation in aquatic environments enriched with SO_4^{2-} ions. Moreover, the proportion of soil-derived humic and highly unsaturated compounds rose from 37% to 60% with the increasing MW of FA samples (Figure S3). A similar trend observed for lignin suggests their dominant roles in complexing ions in NBC-ions-FA solutions. Furthermore, FA-5, with the highest percentage of aromatic components (17%) among the five FA fractions (Figure S4), exhibited distinctive mitigation performance in the ternary solutions. Since both our observation and documented literature agree that FA's aromaticity increases with its MW (Reemtsma et al., 2008), it can be proposed that the aromatic compounds can also play a significant role in mitigating NBC aggregation, even if their content is not particularly high.

Based on the D_h, 3D-EEM, PARAFAC, and FTICR-MS analyses, it can be concluded that the mitigation of NBC aggregation in the NBC-ions-FA solution results from complex interactions among all presenting consents. However, lignin and aromatic substances, are identified as major components in DOMs (FA) that moderate NBC aggregation. Oppositely, the condensed aromatic structures exhibited a negligible effect due to their low abundance.

DFT calculations were further utilized to comparatively tackle the limited resolution of bulk organic analyses, also to elucidate the molecular interactions between FA and ions in the NBC-ions-FA ternary systems. According to the above investigations, FA, HA, tryptophan, tyrosine, and lignin substances are identified as the key DOM compounds that prevent the aggregation of NBC in NBC-ions-FA solutions. Notably, the model structures of FA and HA were divided into three and four structures according to the FTICR-MS analysis. The simulation results are displayed as electrostatic potential (ESP) maps in **Figure 6**, featuring the electrostatic potential and single point charge between ions and the selected 10 model structures. The potential reaction sites were predicted based on the single-point charge values.

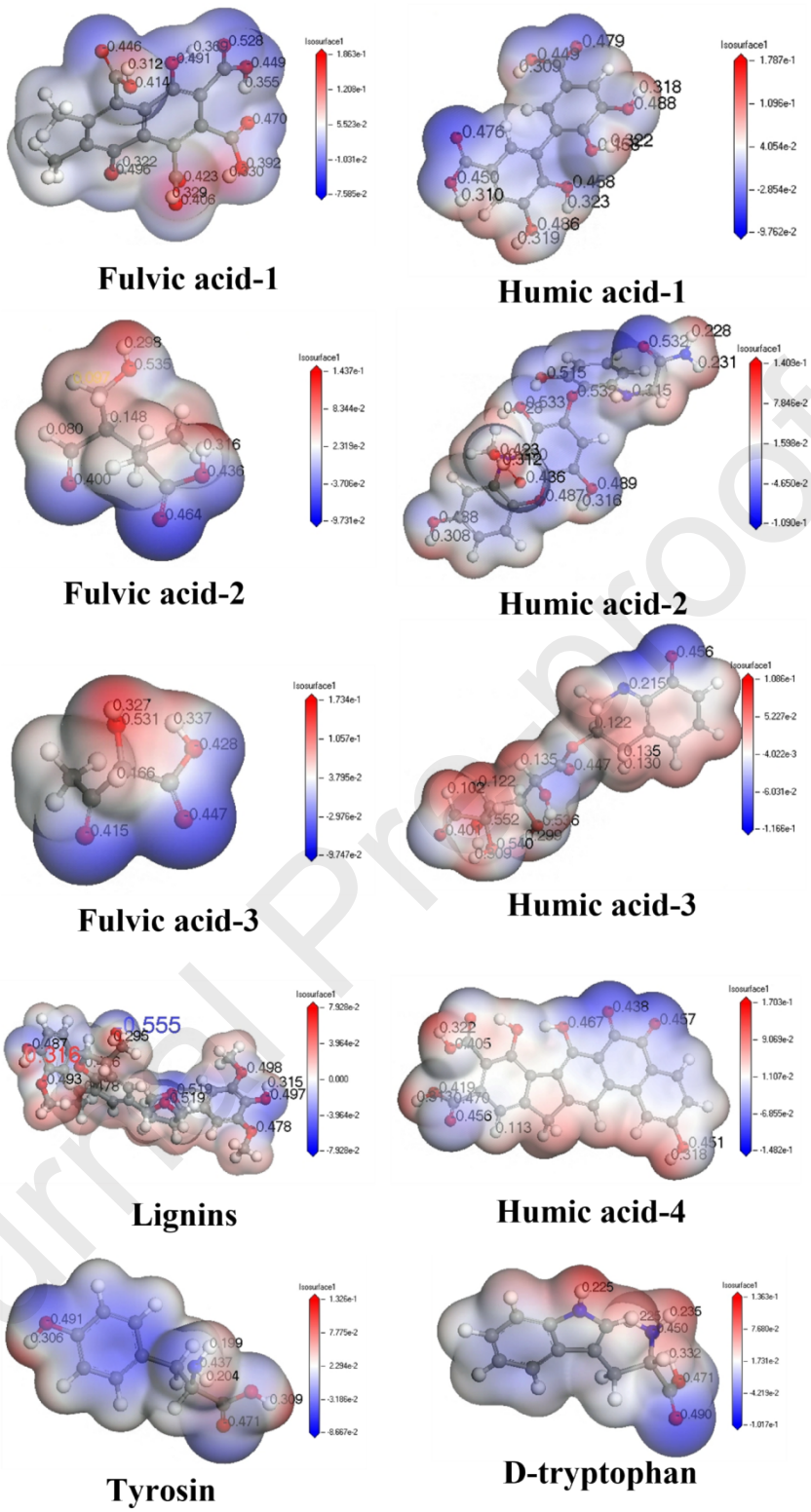

Figure 6. Molecular structural, electron clouds and single-point charge diagrams of model organic substance structures. The blue and red color represents the positive and negative electron clouds, respectively. The shade of the color represents the change in charge density.

As shown in **Figure 6**, the carbonyl and ketone groups displayed the highest negative charges, making them favorable sites for bonding with cations. In contrast, the hydroxyl group exhibited the highest positive charges, tending to complex with anions. Experimental evaluations suggested that HA-like substances have a more significant mitigation effect on NBC than FA-like substances. Based on the simulated molecular structures, it can be concluded that the HA-like substances possess more sites for ion complexations, which ultimately affects the ion-modulated NBC aggregation. In addition, HA-like substances contain abundant ring-like structures, where ion-π interactions could also contribute to the ion complexation. Since these ring structures primarily determine aromaticity of the HA-like substances, this confirms the FTICR-MS results that the aromatic substances can complex with ions and thus moderate the NBC aggregation.

Table 2 displays the interaction energy between each ion and representative substance (The larger values are highlighted in bold). The strongest interaction energies for cations are observed for Na^+-Lignins (-0.5514 eV) and Ca^{2+}-Lignins (-2.0946 eV), while for anions, they are Cl^- - FA-1 (-1.0072 eV) and SO_4^{2-} - FA-1 (-4.9986 eV). The interaction energy demonstrates that lignins, fulvic acid-like and humic acid-like substances complex with ions, consisting with the result from PARAFAC and FTICR-MS. This also confirms that the complexation between ions and organic matters is spontaneous interaction. Additionally, the structure of these substances verifies the critical role of aromatic compounds identified in the previous analyses.

Table 2. The interaction energies between 10 structural models of organic matter and 4 representative ions.

Matters	E(eV)	Matters	E(eV)
Na^++D-tryptophan	-0.1966	Cl^-+D-tryptophan	-0.1580
Na^++Tyrosin	-0.0868	Cl^-+Tyrosin	-0.4096
Na^++Lignins	**-0.5514**	**Cl^-+ Lignins**	**-0.9074**
Na^++Fulvic acid 1	-0.1641	**Cl^-+Fulvic acid 1**	**-1.0072**
Na^++Fulvic acid 2	-0.1764	Cl^-+Fulvic acid 2	-0.4201
Na^++Fulvic acid 3	-0.3322	Cl^-+Fulvic acid 3	-0.4475

Na^++Humic acid 1	-0.1817	Cl^-+Humic acid 1	-0.4716
Na^++Humic acid 2	-0.2220	Cl^-+Humic acid 2	-0.3789
Na^++Humic acid 3	-0.1786	Cl^-+Humic acid 3	-0.4921
Na^++Humic acid 4	**-0.4095**	Cl^-+Humic acid 4	-0.4735
Ca^{2+}+D-tryptophan	**-1.9621**	SO_4^{2-}+D-tryptophan	-0.0158
Ca^{2+}+Tyrosin	-0.5897	SO_4^{2-}+Tyrosin	-0.8961
Ca^{2+}+ Lignins	**-2.0946**	SO_4^{2-}+ Lignins	-1.0588
Ca^{2+}+Fulvic acid 1	-1.1427	**SO_4^{2-}+Fulvic acid 1**	**-4.9986**
Ca^{2+}+Fulvic acid 2	-0.9663	SO_4^{2-}+Fulvic acid 2	-1.0707
Ca^{2+}+Fulvic acid 3	-1.5536	SO_4^{2-}+Fulvic acid 3	-0.7643
Ca^{2+}+Humic acid 1	-1.0650	SO_4^{2-}+Humic acid 1	-1.0661
Ca^{2+}+Humic acid 2	-1.1466	SO_4^{2-}+Humic acid 2	-0.8768
Ca^{2+}+Humic acid 3	-1.0629	SO_4^{2-}+Humic acid 3	-0.7252
Ca^{2+}+Humic acid 4	**-1.9028**	**SO_4^{2-}+Humic acid 4**	**-3.3082**

3.5 Discussions on the future perspectives in regulating NBC aggregation

When NBC is dispersed in pure water, the negative charge on its surface facilitates its stable suspension due to balanced electrostatic repulsion and van der Waals forces. However, the application of NBC in real aquatic environments has many challenges, including the presence of coexisting ions and DOMs (**Figure 7**). The evaluations above thus provide potential strategies for regulating NBC's functional efficacy and associated ecological risks.

In this study, DOMs were fractionated into different MWs to evaluate their distinguishable effect on moderating NBC aggregation. However, DOMs exist in

actual water bodies in a united form. The pre-assessment of existing DOM components can be beneficial before implementing the NBC, particularly the key regulation components of aromatic compounds and unsaturated hydrocarbons, which require significant attention. Considering the convenience of sample testing, a fluorescence scan can quickly identify the bulk DOM matrix of the humic acid-like and FA-like substances, enabling the development of a targeted NBC aggregation regulation strategy. In scenarios involving heavy metals, the strong complexation affinity between NBC and metal cations raises concerns, as these metal ions can be transported alongside NBC due to their small size (Wang et al., 2013a). In such cases, aggregation of NBC is preferred, requiring control over the abundance of aromatic compounds at application sites. This can decrease the mobility, leachability, and availability of heavy metals, thereby preventing the potential uptake of toxic elements (Gong et al., 2022). Conversely, certain situations may require promoting NBC aggregation. For instance, treating highly concentrated pollution sources would benefit from regulating NBC aggregation to ensure adequate contact with targeted contaminants. In these instances, additional injection of aromatic compounds may be advantageous. However, the ion and DOM concentrations in actual water bodies may not reach the CCC concentrations obtained in our experiments, resulting in a limited promoting effect on NBC aggregation (Yang et al., 2019). Therefore, pre-evaluation of complex substances in actual environments can help optimize the tailored dosage of NBC and regulatory additives, particularly for the *in-situ* remediation of specific contaminants.

It is crucial to consider the aging and recycling of NBC once applied to the environment (Palansooriya et al., 2020; Wang et al., 2019), in particular, recognizing the potential damage caused by improper biochar use. For instance, long-term biochar application may alter heavy metal transport in soil, reducing Cd concentrations but increasing Pb levels (Fan et al., 2020). It is demonstrated that biochar application could contaminate plants with PAHs, posing risks to human health (Wang et al., 2018). The generation of persistent free radicals by biochar is another critical factor to consider when assessing ecological impacts (Odinga et al., 2020). Developing a framework for rapid evaluation of NBC aggregation and migration in environmental media could offer valuable insights for its practical applications.

The presence of multiple ions and contaminants, as well as other NBC carriers, may complicate the scenario after NBC addition. On the one hand, our observations were obtained in a relatively pure solution matrix. In real water environments with high concentrations of organic pollutants, the interactions between contaminants and DOMs may reduce NBC functioning efficacy due to the fouling effect of DOMs on the NBC surface (Shimabuku et al., 2016). The coexistence of low molecular weight organic acids (LMWOAs) with DOMs and NBC may reduce the moderating of NBC aggregation by DOMs. LMWOAs can enhance NBC aggregation by increasing hydrogen bonding and decreasing the repulsive forces between NBC particles (Wang et al., 2022). In the presence of heavy metals, ions, DOMs, and NBC, the metal adsorption capacity of NBC may be hindered due to the strong interactions between

heavy metals and DOMs, facilitating the potential migration of mobilizable heavy metals (Chaudhuri et al., 2022). Additionally, our observation indicates that aromatic substances in DOM can regulate NBC aggregation effectively. Since the primary pathway of aromatic organic pollutants adsorbed by NBC and DOMs is π - π interaction (Li et al., 2020), this raises concerns about their migration in aquatic environments after sorption. Consequently, the application of NBC should be executed on a *case-by-case* basis, considering the complex aquatic environments. On the other hand, advancing high-resolution organic characterization techniques, alongside customizable modifications of NBC, offer promising future directions for the effective deployment of NBC in pollution control. In summary, we propose mechanisms that regulate the aggregation of nano-biochar particles in aqueous solutions.

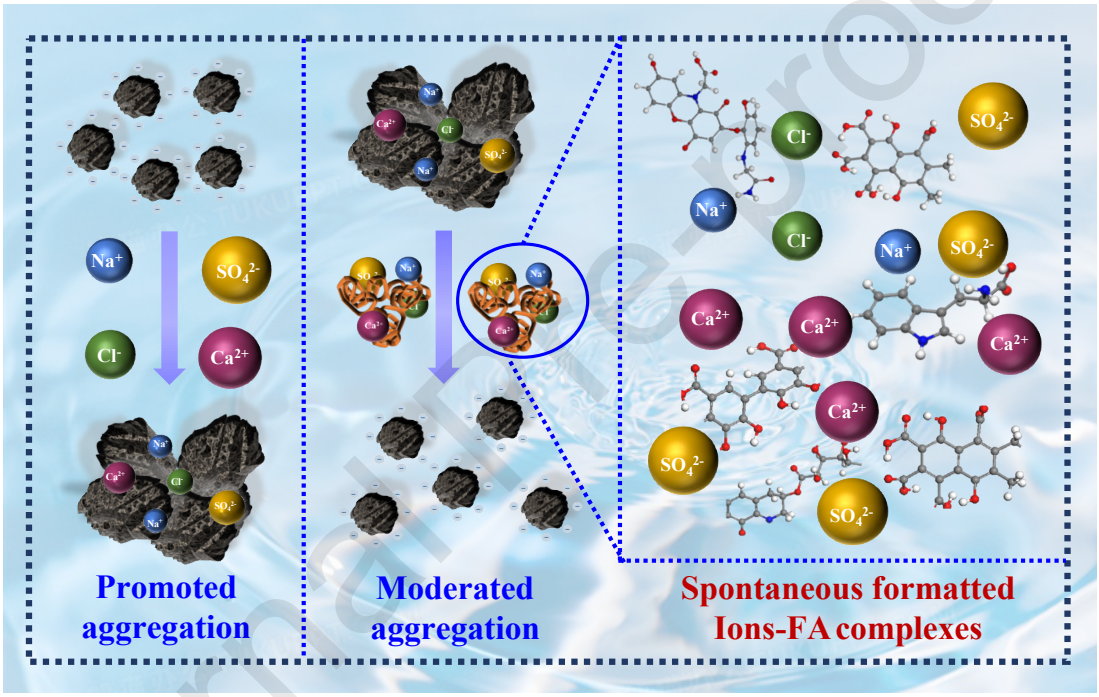

Figure 7. Schematic diagram of the NBC aggregation in the presence of ions and moderated by aromatic components in DOM.

4. Conclusion

This study demonstrated the behaviors and mechanisms of NBC aggregation in aquatic environments containing electrolytes and dissolved organic matter through a combined experimental and simulation approach. Mono/di-valent electrolytes promote NBC aggregation with a critical aggregation concentration of 492.8 mM Na^+, 37.9 mM Ca^{2+}, and 109.4 mM SO_4^{2-}. After adding FA, NBC aggregation is effectively moderated, with higher molecular weight FA fractions showing better performance. Humic acid-like substances, followed by FA-like substances, particularly aromatic

substances, are identified as the dominant compounds moderating NBC aggregation in NBC-ions-FA solutions. Complexation between aromatic substances and ions (Na^+, Ca^{2+}, Cl^-, and SO_4^{2-}) facilitates the spontaneous formation of ion-FA complexes, reducing ion concentrations in solution through cation bridging and increasing steric effects, thereby effectively reducing NBC aggregation in NBC-ions-FA solutions. From a future perspective, adjusting the content of aromatic substances can regulate NBC aggregation in aquatic environments, maximizing its effectiveness and minimizing potential ecological risks. This provides regulation strategies for precise, efficient, and low-risk nano-biochar applications. Ultimately, this study provides insights into the aggregation and migration of nanoparticles in aquatic environments.

Notes

The authors declare no competing financial interest.

Acknowledgments

This research was supported by the National Natural Science Foundation of China (42130711, 42277399, 42307499, and 42467031), Yunnan Major Scientific and Technological Projects (202202AG050019).

References

Chaudhuri, S.; Sigmund, G.; Bone, S. E.; Kumar, N.; Hofmann, T. 2022. Mercury Removal from Contaminated Water by Wood-Based Biochar Depends on Natural Organic Matter and Ionic Composition. Environmental Science & Technology. 56:11354-11362; 10.1021/acs.est.2c01554

Chen, M.; Wang, D.; Yang, F.; Xu, X.; Xu, N.; Cao, X. 2017. Transport and retention of biochar nanoparticles in a paddy soil under environmentally-relevant solution chemistry conditions. Environmental Pollution. 230:540-549; 10.1016/j.envpol.2017.06.101

Chen, W.; Yu, H.-Q. 2021. Advances in the characterization and monitoring of natural organic matter using spectroscopic approaches. Water Research. 190:116759; 10.1016/j.watres.2020.116759

D.Schmitt, H. E. T., G.R. Aiken. 2002. Influence of Natural Organic Matter on the Adsorption of Metal Ions onto Clay Minerals. Environmental Science & Technology. 36:2932-2938; 10.1021/es010271p

Devarajan, D.; Liang, L.; Gu, B.; Brooks, S. C.; Parks, J. M.; Smith, J. C. 2020. Molecular Dynamics Simulation of the Structures, Dynamics, and Aggregation of Dissolved Organic Matter.

Environmental Science & Technology. 54:13527-13537; 10.1021/acs.est.0c01176

Fan, Q.; Sun, J.; Quan, G.; Yan, J.; Gao, J.; Zou, X.; Cui, L. 2020. Insights into the effects of long-term biochar loading on water-soluble organic matter in soil: Implications for the vertical co-migration of heavy metals. Environment International. 136:105439; 10.1016/j.envint.2019.105439

Fang, Q.; Chen, B.; Lin, Y.; Guan, Y. 2013. Aromatic and Hydrophobic Surfaces of Wood-derived Biochar Enhance Perchlorate Adsorption via Hydrogen Bonding to Oxygen-containing Organic Groups. Environmental Science & Technology. 48:279-288; 10.1021/es403711y

Gao, Y.; Ren, X.; Tan, X.; Hayat, T.; Alsaedi, A.; Chen, C. 2017. Insights into key factors controlling GO stability in natural surface waters. Journal of Hazardous Materials. 335:56-65; 10.1016/j.jhazmat.2017.04.027

Gong, H.; Zhao, L.; Rui, X.; Hu, J.; Zhu, N. 2022. A review of pristine and modified biochar immobilizing typical heavy metals in soil: Applications and challenges. Journal of Hazardous Materials. 432:128668; 10.1016/j.jhazmat.2022.128668

Hagemann, N.; Joseph, S.; Schmidt, H.-P.; Kammann, C. I.; Harter, J.; Borch, T.; Young, R. B.; Varga, K.; Taherymoosavi, S.; Elliott, K. W.; McKenna, A.; Albu, M.; Mayrhofer, C.; Obst, M.; Conte, P.; Dieguez-Alonso, A.; Orsetti, S.; Subdiaga, E.; Behrens, S.; Kappler, A. 2017. Organic coating on biochar explains its nutrient retention and stimulation of soil fertility. Nature Communications. 8; 10.1038/s41467-017-01123-0

He, M.; Xu, Z.; Hou, D.; Gao, B.; Cao, X.; Ok, Y. S.; Rinklebe, J.; Bolan, N. S.; Tsang, D. C. W. 2022. Waste-derived biochar for water pollution control and sustainable development. Nature Reviews Earth & Environment. 3:444-460; 10.1038/s43017-022-00306-8

Hu, F.; Xu, C.; Ma, R.; Tu, K.; Yang, J.; Zhao, S.; Yang, M.; Zhang, F. 2021. Biochar application driven change in soil internal forces improves aggregate stability: Based on a two-year field study. Geoderma. 403:115276; 10.1016/j.geoderma.2021.115276

Huang, F.; Xiao, l.; Jiang, J.; Ma, J.; Liu, Y.; Yang, J. 2013. Aggregation Kinetics of Manganese Dioxide Colloids in Aqueous Solution: Influence of Humic Substances and Biomacromolecules. Environmental Science & Technology. 47:10285-10292; 10.1021/es4003247

Huguet, A.; Vacher, L.; Relexans, S.; Saubusse, S.; Froidefond, J. M.; Parlanti, E. 2009. Properties of fluorescent dissolved organic matter in the Gironde Estuary. Organic Geochemistry. 40:706-719; 10.1016/j.orggeochem.2009.03.002

Jiang, M.; He, L.; Niazi, N. K.; Wang, H.; Gustave, W.; Vithanage, M.; Geng, K.; Shang, H.; Zhang, X.; Wang, Z. 2023. Nanobiochar for the remediation of contaminated soil and water: challenges and opportunities. Biochar. 5; 10.1007/s42773-022-00201-x

Jin, Z.; Xiao, S.; Dong, H.; Xiao, J.; Tian, R.; Chen, J.; Li, Y.; Li, L. 2022. Adsorption and catalytic

degradation of organic contaminants by biochar: Overlooked role of biochar's particle size. Journal of Hazardous Materials. 422:126928; 10.1016/j.jhazmat.2021.126928

Li, Q.; Chen, B.; Xing, B. 2017. Aggregation Kinetics and Self-Assembly Mechanisms of Graphene Quantum Dots in Aqueous Solutions: Cooperative Effects of pH and Electrolytes. Environmental Science & Technology. 51:1364-1376; 10.1021/acs.est.6b04178

Li, R.; Zhang, Y.; Deng, H.; Zhang, Z.; Wang, J. J.; Shaheen, S. M.; Xiao, R.; Rinklebe, J.; Xi, B.; He, X.; Du, J. 2020. Removing tetracycline and Hg(II) with ball-milled magnetic nanobiochar and its potential on polluted irrigation water reclamation. Journal of Hazardous Materials. 384:121095; 10.1016/j.jhazmat.2019.121095

Li, Y.; Harir, M.; Lucio, M.; Gonsior, M.; Koch, B. P.; Schmitt-Kopplin, P.; Hertkorn, N. 2016. Comprehensive structure-selective characterization of dissolved organic matter by reducing molecular complexity and increasing analytical dimensions. Water Research. 106:477-487; 10.1016/j.watres.2016.10.034

Lian, F.; Gu, S.; Han, Y.; Wang, Z.; Xing, B. 2022. Novel Insights into the Impact of Nano-Biochar on Composition and Structural Transformation of Mineral/Nano-Biochar Heteroaggregates in the Presence of Root Exudates. Environmental Science & Technology. 56:9816-9825; 10.1021/acs.est.2c02127

Lian, F.; Xing, B. 2024. From Bulk to Nano: Formation, Features, and Functions of Nano-Black Carbon in Biogeochemical Processes. Environmental Science & Technology. 58:15910-15925; 10.1021/acs.est.4c07027

Lian, F.; Yu, W.; Zhou, Q.; Gu, S.; Wang, Z.; Xing, B. 2020. Size Matters: Nano-Biochar Triggers Decomposition and Transformation Inhibition of Antibiotic Resistance Genes in Aqueous Environments. Environmental Science & Technology. 54:8821-8829; 10.1021/acs.est.0c02227

Lin, M. Y.; Lindsay, H. M.; Weitz, D. A.; Ball, R. C.; Klein, R.; Meakin, P. 1990. Universal reaction-limited colloid aggregation. Physical Review A. 41:2005-2020; 10.1103/PhysRevA.41.2005

Lin, X.; Lu, G.; Wu, M.; Cheng, Z.; Hao, Y.; Mo, C.; Li, Q.; Wu, J.; Wu, J.; Hu, B. X. 2023. Determining the transport behaviors of biochar nano-particles in porous media. Chemical Engineering Research and Design. 199:676-688; 10.1016/j.cherd.2023.09.045

Liu, G.; Zheng, H.; Jiang, Z.; Zhao, J.; Wang, Z.; Pan, B.; Xing, B. 2018. Formation and Physicochemical Characteristics of Nano Biochar: Insight into Chemical and Colloidal Stability. Environmental Science & Technology. 52:10369-10379; 10.1021/acs.est.8b01481

Liu, P.; Ptacek, C. J.; Blowes, D. W.; Finfrock, Y. Z.; Liu, Y. 2020. Characterization of chromium species and distribution during Cr(VI) removal by biochar using confocal micro-X-ray fluorescence redox mapping and X-ray absorption spectroscopy. Environment International. 134:105216; 10.1016/j.envint.2019.105216

Liu, Y.; Ma, J.; Gao, J.; Chen, X.; Ouyang, X.; Weng, L.; Li, H.; Chen, Y.; Li, Y. 2022. Stability and interaction of biochar and iron mineral nanoparticles: effect of pH, ionic strength, and dissolved organic matter. Biochar. 4; 10.1007/s42773-022-00172-z

Lu, Q.; Wang, Z.; Wang, J.; Xie, L.; Liu, Q.; Zeng, H. 2023. Deciphering the specific interaction of humic acid with divalent cations at the nanoscale. Chemical Engineering Journal. 470:144097; 10.1016/j.cej.2023.144097

Lu, Y.; Cai, Y.; Zhang, S.; Zhuang, L.; Hu, B.; Wang, S.; Chen, J.; Wang, X. 2022. Application of biochar-based photocatalysts for adsorption-(photo)degradation/reduction of environmental contaminants: mechanism, challenges and perspective. Biochar. 4; 10.1007/s42773-022-00173-y

Maizel, A. C.; Remucal, C. K. 2017. The effect of advanced secondary municipal wastewater treatment on the molecular composition of dissolved organic matter. Water Research. 122:42-52; 10.1016/j.watres.2017.05.055

Naghdi, M.; Taheran, M.; Brar, S. K.; Kermanshahi-pour, A.; Verma, M.; Surampalli, R. Y. 2018. Pinewood nanobiochar: A unique carrier for the immobilization of crude laccase by covalent bonding. International Journal of Biological Macromolecules. 115:563-571; 10.1016/j.ijbiomac.2018.04.105

Naghdi, M.; Taheran, M.; Brar, S. K.; Rouissi, T.; Verma, M.; Surampalli, R. Y.; Valero, J. R. 2017. A green method for production of nanobiochar by ball milling- optimization and characterization. Journal of Cleaner Production. 164:1394-1405; 10.1016/j.jclepro.2017.07.084

Norbert, K.; Norbert, H.; Mourad, H. 2019. Molecular change of dissolved organic matter and patterns of bacterial activity in a stream along a land-use gradient. Water Research. 164; 10.1016/j.watres.2019.114919

Odinga, E. S.; Waigi, M. G.; Gudda, F. O.; Wang, J.; Yang, B.; Hu, X.; Li, S.; Gao, Y. 2020. Occurrence, formation, environmental fate and risks of environmentally persistent free radicals in biochars. Environment International. 134:105172; 10.1016/j.envint.2019.105172

Palansooriya, K. N.; Shaheen, S. M.; Chen, S. S.; Tsang, D. C. W.; Hashimoto, Y.; Hou, D.; Bolan, N. S.; Rinklebe, J.; Ok, Y. S. 2020. Soil amendments for immobilization of potentially toxic elements in contaminated soils: A critical review. Environment International. 134:105046; 10.1016/j.envint.2019.105046

Qiu, B.; Shao, Q.; Shi, J.; Yang, C.; Chu, H. 2022. Application of biochar for the adsorption of organic pollutants from wastewater: Modification strategies, mechanisms and challenges. Separation and Purification Technology. 300:121925; 10.1016/j.seppur.2022.121925

Reemtsma, T.; These, A.; Springer, A.; Linscheid, M. 2008. Differences in the molecular composition of fulvic acid size fractions detected by size-exclusion chromatography–on line Fourier transform ion cyclotron resonance (FTICR–) mass spectrometry. Water Research. 42:63-72;

10.1016/j.watres.2007.06.063

Rosenberg, Y. O.; Metz, V.; Oren, Y.; Volkman, Y.; Ganor, J. 2011. Co-precipitation of radium in high ionic strength systems: 2. Kinetic and ionic strength effects. Geochimica et Cosmochimica Acta. 75:5403-5422; 10.1016/j.gca.2011.07.013

Shao, Z.; Luo, S.; Liang, M.; Ning, Z.; Sun, W.; Zhu, Y.; Mo, J.; Li, Y.; Huang, W.; Chen, C. 2021. Colloidal stability of nanosized activated carbon in aquatic systems: Effects of pH, electrolytes, and macromolecules. Water Research. 203:117561; 10.1016/j.watres.2021.117561

Shimabuku, K. K.; Kearns, J. P.; Martinez, J. E.; Mahoney, R. B.; Moreno-Vasquez, L.; Summers, R. S. 2016. Biochar sorbents for sulfamethoxazole removal from surface water, stormwater, and wastewater effluent. Water Research. 96:236-245; 10.1016/j.watres.2016.03.049

Singh, N.; Khandelwal, N.; Ganie, Z. A.; Tiwari, E.; Darbha, G. K. 2021. Eco-friendly magnetic biochar: An effective trap for nanoplastics of varying surface functionality and size in the aqueous environment. Chemical Engineering Journal. 418:129405; 10.1016/j.cej.2021.129405

Song, B.; Cao, X.; Gao, W.; Aziz, S.; Gao, S.; Lam, C.-H.; Lin, R. 2022. Preparation of nano-biochar from conventional biorefineries for high-value applications. Renewable and Sustainable Energy Reviews. 157:112057; 10.1016/j.rser.2021.112057

Song, Q.; Kong, F.; Liu, B.-F.; Song, X.; Ren, H.-Y. 2024. Biochar-based composites for removing chlorinated organic pollutants: Applications, mechanisms, and perspectives. Environmental Science and Ecotechnology. 21:100420; 10.1016/j.ese.2024.100420

TANAPON, P.; NAVID, S.; KEVIN, S.; TILTON, R. D. 2007. Aggregation and sedimentation of aqueous nanoscale zerovalent iron dispersions. Environmental Science & Technology. 41:284-290; 10.1021/es061349a

Wang, D.; Zhang, W.; Hao, X.; Zhou, D. 2013a. Transport of Biochar Particles in Saturated Granular Media: Effects of Pyrolysis Temperature and Particle Size. Environmental Science & Technology. 47:821-828; 10.1021/es303794d

Wang, D.; Zhang, W.; Zhou, D. 2013b. Antagonistic Effects of Humic Acid and Iron Oxyhydroxide Grain-Coating on Biochar Nanoparticle Transport in Saturated Sand. Environmental Science & Technology. 47:5154-5161; 10.1021/es305337r

Wang, J.; Xia, K.; Waigi, M. G.; Gao, Y.; Odinga, E. S.; Ling, W.; Liu, J. 2018. Application of biochar to soils may result in plant contamination and human cancer risk due to exposure of polycyclic aromatic hydrocarbons. Environment International. 121:169-177; 10.1016/j.envint.2018.09.010

Wang, Y.; Wang, C.; Xiong, J.; Zhang, Q.; Shang, J. 2022. Effects of low molecular weight organic acids on aggregation behavior of biochar colloids at acid and neutral conditions. Biochar. 4; 10.1007/s42773-022-00142-5

Wang, Y.; Zhang, W.; Shang, J.; Shen, C.; Joseph, S. D. 2019. Chemical Aging Changed Aggregation Kinetics and Transport of Biochar Colloids. Environmental Science & Technology. 53:8136-8146; 10.1021/acs.est.9b00583

Wei, S.; Li, Z.; Sun, Y.; Zhang, J.; Ge, Y.; Li, Z. 2022. A comprehensive review on biomass humification: Recent advances in pathways, challenges, new applications, and perspectives. Renewable and Sustainable Energy Reviews. 170:112984; 10.1016/j.rser.2022.112984

Xing, J.; Qi, Z.; Dong, W.; Chen, Q.; Wu, M.; Yi, P.; Pan, B.; Xing, B. 2023. Aggregation of biochar nanoparticles and the impact on bisphenol A sorption: Experiments and molecular dynamics simulations. Science of The Total Environment. 875:162724; 10.1016/j.scitotenv.2023.162724

Xu, Y.; Ou, Q.; He, Q.; Wu, Z.; Ma, J.; Huangfu, X. 2021. Influence of dissolved black carbon on the aggregation and deposition of polystyrene nanoplastics: Comparison with dissolved humic acid. Water Research. 196:117054; 10.1016/j.watres.2021.117054

Yang, F.; Antonietti, M. 2020. The sleeping giant: A polymer View on humic matter in synthesis and applications. Progress in Polymer Science. 100:101182; 10.1016/j.progpolymsci.2019.101182

Yang, W.; Li, B.; Shang, J. 2022. Aggregation kinetics of biochar nanoparticles in aqueous environment: Interplays of anion type and bovine serum albumin. Science of The Total Environment. 833:155148; 10.1016/j.scitotenv.2022.155148

Yang, W.; Shang, J.; Li, B.; Flury, M. 2019. Surface and colloid properties of biochar and implications for transport in porous media. Critical Reviews in Environmental Science and Technology. 50:2484-2522; 10.1080/10643389.2019.1699381

Zhang, X.; Wells, M.; Niazi, N. K.; Bolan, N.; Shaheen, S.; Hou, D.; Gao, B.; Wang, H.; Rinklebe, J.; Wang, Z. 2022. Nanobiochar-rhizosphere interactions: Implications for the remediation of heavy-metal contaminated soils. Environmental Pollution. 299:118810; 10.1016/j.envpol.2022.118810

Highlights:

1. NBC aggregation is controlled by Van der Waals forces and electrostatic repulsion.
2. FA fractions with higher molecular weights can effectively moderate NBC aggregation.
3. Lignin with aromatic structures are key components in moderating NBC aggregation.
4. Aromatic structures in FA can spontaneously form complexes with electrolytes.

Graphical Abstract

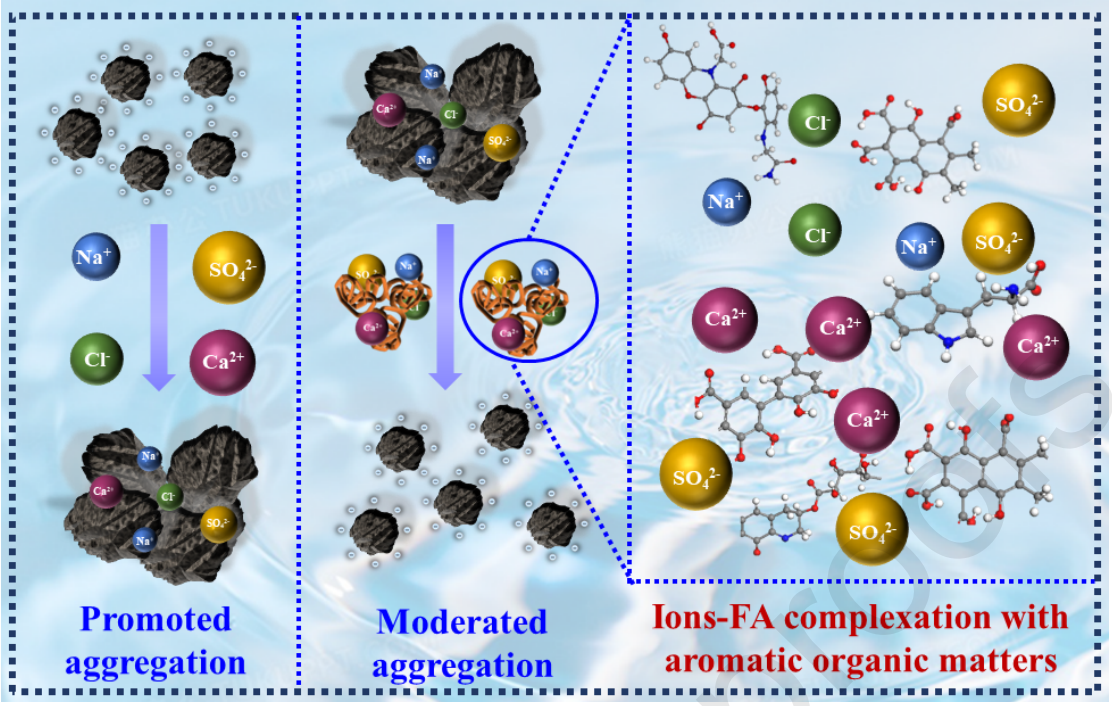

Schematic diagram of the NBC aggregation in the presence of ions and moderated by aromatic components in DOM.